

Title No. 121-S59

Shear Strength Equation and Database for High-Strength High-Performance Fiber-Reinforced Concrete and Ultra-High-Performance Concrete Beams without Stirrups

by Manuel Bermudez and Chung-Chan Hung

The study presented a shear strength equation for high-strength high-performance fiber-reinforced concrete (HS-HPFRC), including ultra-high-performance concrete (UHPC). This equation was designed for straightforward implementation, catering to the regular tasks of engineers. It considers various influences on shear-transfer mechanisms, including fiber bridging, fiber distribution, dowel action, cross-sectional shapes, and beam size effects. The equation does not rely on uniaxial tensile tests or inverse analysis of flexural tests; instead, it considers the statistical impact of fibers on shear strength. To generate the coefficients for this semi-empirical closed-form equation, an evaluation database of 118 HS-HPFRC and UHPC beams was constructed. The evaluation results revealed that the proposed equation has a mean of 1.00 and a correlation coefficient of 0.92, indicating low variation and high predictive accuracy. Furthermore, it outperformed existing equations and matched the accuracy of the machine learning (ML)-based models including support vector machines (SVM), random forest (RF), and artificial neural network (ANN), despite its comparatively simpler expression.

Keywords: beam shape; closed-form equation; fiber distribution; high-performance fiber-reinforced concrete (HPFRC); hybrid fibers; machine learning (ML); shear-transfer mechanism; size effect; ultra-high-performance concrete (UHPC).

INTRODUCTION

High-strength high-performance fiber-reinforced concrete (HS-HPFRC), including ultra-high-performance concrete (UHPC), exhibits tensile strain-hardening behavior, high ductility, and high compressive strength. The fiber bridging effect in HS-HPFRC and UHPC materials leads to a post-cracking strength greater than the initial crack strength, enabling tensile stress redistribution and enhancing shear strength.¹⁻⁴ Existing studies^{3,5} demonstrated that HS-HPFRC and UHPC beams with shear span-effective depth ratio (a/d) greater than 2.5 had a normalized concrete shear capacity that is at least double that of conventional concrete per ACI 318-19.⁶ The high shear strength of HS-HPFRC and UHPC beams opens the possibility of structural optimizations.^{1,4,7-10}

The shear strength of HS-HPFRC and UHPC beams without stirrups is closely related to the tensile strength of concrete, especially when beam action predominantly governs the shear-transfer mechanism. However, there are still concerns about the current test methods for determining the tensile properties of HS-HPFRC and UHPC. A common method to determine the tensile strength of HS-HPFRC and UHPC is the uniaxial tensile test. Although there are

several standards for uniaxial tensile tests on dog bone-shaped and prismatic specimens,¹¹⁻¹³ debates continue about the geometry and dimensions of the specimens as well as the test setup. In addition, conducting and interpreting these tests require high technical expertise, creating obstacles in generalizing the method. This is evident as only 31% of 222 nonprestressed HS-HPFRC and UHPC beams tested in past studies^{1,5,7-10,14-39} reported the direct tensile strength of the material.

Design guidelines and standards from France,⁴⁰ Switzerland,¹² and Canada^{41,42} adopt inverse analysis of a flexural test to obtain the residual tensile strength of HS-HPFRC and UHPC for shear strength prediction. Standards such as ASTM C1609 and EN 14651 can be followed to conduct flexural tests, but these generate high variability⁴³ in FRC's residual tensile strength. Furthermore, Bencardino et al.⁴³ highlighted critical issues regarding flexural test procedures. Another crucial consideration is the inherent heterogeneity and anisotropy of HS-HPFRC and UHPC. This presents a challenge in directly correlating the shear strength at the structural scale with the tensile strength at the material scale.

This study aims to develop a reasonably accurate, reliable, and yet simple shear strength equation for nonprestressed HS-HPFRC and UHPC beams without stirrups. Rather than resorting to uniaxial tensile tests or inverse analysis of flexural tests, the equation incorporates semi-empirical factors to consider the statistical impact of fibers on beam shear strength. The predictive performance of the strength equation was evaluated by comparing it with existing shear strength equations and three newly developed machine learning (ML)-based models that were trained to optimize their prediction performance based on the established database.

RESEARCH SIGNIFICANCE

Shear strength equations for HS-HPFRC and UHPC are in design guidelines and standards^{12,40-42} but depend on tensile strength tests or inverse analysis of flexural tests, which are complex and challenging due to material heterogeneity and anisotropy. This study developed a simpler shear strength equation for HS-HPFRC and UHPC beams. Factors

ACI Structural Journal, V. 121, No. 4, July 2024.

MS No. S-2023-235.R1, doi: 10.14359/51740716, received January 5, 2024, and reviewed under Institute publication policies. Copyright © 2024, American Concrete Institute. All rights reserved, including the making of copies unless permission is obtained from the copyright proprietors. Pertinent discussion including author's closure, if any, will be published ten months from this journal's date if the discussion is received within four months of the paper's print publication.

Table 1—Filtering criteria for database of nonprestressed HS-HPFRC and UHPC beams

Data filters (DFs)		Criteria	Fulfilled	Unfulfilled
Materials	1	$f'_{c,cylinder} \geq 80 \text{ MPa (11.6 ksi)}$	222	0
	2	$\sigma_p > \sigma_c$	222	0
Dimensions	3	$b_w = b \geq 30 \text{ mm (1.18 in.)}$	222	0
	4	$h > 70 \text{ mm (2.76 in.)}$	222	0
Damage patterns	5	Evidence of shear failure	136	86
	6	$V_{u,test}/V_{mn,ACI318} < 1.0$	136	86
Data adequacy	7	All required design parameters for proposed equation are provided	204	18
Evaluation database	Combination of critical criteria (fulfilled-unfulfilled)		118	104

including fiber bridging, dowel action, cross-sectional shapes, and size effects were considered. The equation was optimized using an established database of HS-HPFRC and UHPC beams. The proposed equation only relies on available design parameters, avoiding tensile and flexural tests. This offers a reliable tool for HS-HPFRC and UHPC design.

ESTABLISHMENT OF SHEAR DATABASE OF NONPRESTRESSED HS-HPFRC AND UHPC BEAMS WITHOUT STIRRUPS

Shear tests on FRC beams^{1,7-10,14-39} have been conducted to investigate the influences of fibers, a/d , coarse aggregate, and so on. In this study, a qualified database for the shear strength of HS-HPFRC and UHPC beams was established to provide an adequate subset for data-driven approaches. The collection database contained 222 shear tests on HS-HPFRC and UHPC beams.^{1,5,7-10,14-39} Then, the filtering criteria employed by Joint ACI-ASCE Committee 445^{44,45} were modified and implemented to ensure the quality of the shear database for HS-HPFRC and UHPC beams. Table 1 summarizes the seven data filters (DFs) used for the evaluation database. The DFs can be categorized into the criteria associated with materials (DFs 1 and 2), dimensions (DFs 3 and 4), damage patterns (DFs 5 and 6), and data adequacy (DF 7).

DF1 captured HS-HPFRC and UHPC beams with a minimum compressive strength of 80 MPa (11.6 ksi). DF2 filtered out beams with concrete materials not classified as HS-HPFRC or UHPC by the original studies or those lacking evidence of tensile strain hardening. In DF2, the strain hardening criterion was defined by the condition where the post-cracking tensile strength σ_p exceeds the initial cracking strength σ_c .

DF3 is the minimum beam width. While DF3 was set to be 50 mm (1.97 in.) in the RC database,^{44,45} it was reduced to 30 mm (1.18 in.) in the study to account for the ultra-high mechanical properties of HS-HPFRC and UHPC that facilitate structurally optimized cross sections. For DF4, the minimum height of the beams was set to be 70 mm (2.76 in.), as defined in the RC database.^{44,45}

Two strict DFs were employed to ensure that the included beams had a peak strength controlled by diagonal shear damage rather than flexural behavior or other damage patterns. DF5 was implemented to only include the beams that were reported to have shear-critical failures. The figures

of the beams' failure patterns reported by the original authors were evaluated to verify the development of a multiple cracking pattern prior to the formation of shear crack localization. Furthermore, to eliminate the possibility of including beams that had a flexure-shear failure—that is, reaching flexural capacity prior to shear failure—a conservative strength-based filter (that is, DF6: $V_{u,test}/V_{mn,ACI318} < 1.0$) was employed, where $V_{u,test}$ is the peak shear demand obtained by the experimental test, and $V_{mn,ACI318}$ is the shear demand of the beam when the nominal flexural strength is reached. The nominal flexural capacity of the beam ($M_{n,ACI318}$) was calculated according to ACI 318-19.⁶ It should be noted that the calculation ignores the contribution of fibers to the beams' flexural capacity, which usually ranges from 10 to 25%.⁴⁶ As a result, some beams excluded by DF6 could actually have a peak strength governed by shear failure. In the meantime, a closer inspection was conducted on the 222 beams with a $V_{u,test}/V_{mn,ACI318} = 1.0$ to 1.3. The results indicated that several beams in this category displayed obvious flexural cracks prior to the formation of localized shear cracks. Therefore, it was considered reasonable to use the conservative DF6 as it ensures only the beams with a peak strength controlled by shear failure were included in the database. The filtering results show that 136 out of the 222 beams fulfilled both DF5 and DF6.

The last DF, DF7, filtered tested beams with insufficient reported details for deriving the shear equation. Missing information about the beams included the property and volume fraction of fibers, a/d , effective depth, and shear strength.

The qualified database that fulfilled all DFs had 118 beams. Table 2 summarizes the detailed information for the 118 beams and presents the range of values for key parameters. These parameters include the a/d , cross-sectional dimensions, shape of the beams, ρ_w (the ratio of A_s to $b_w d$, where A_s is the area of nonprestressed longitudinal tension reinforcement), cylinder compressive strength f'_c , and the fiber reinforcement. Figure 1 shows the distribution of the beam shear strengths against different design parameters. The data set included 81 rectangular beams, 33 I-shaped beams, and four T-shaped beams. The compressive strengths presented in Table 2 were cylinder strengths. The conversion factors of Graybeal and Davis⁴⁷ for cubes to cylinders were used when the studies did not report the strength of both cylinders and cubes. The average compressive strength in

Table 2—Evaluation shear database of nonprestressed HS-HPFRC and UHPC beams

Reference	No. of beams	Shape	b , mm	b_w , mm	d , mm	a/d	ρ_w , %	f'_c , MPa	V_f , %	v_u , MPa
Ashour et al. ¹⁴	5	R	125	125	215	1.0 to 4.0	2.8 to 4.6	94 to 99	0.5 to 1.0	2.3 to 9.1
Shin et al. ¹⁵	3	R	100	100	175	3.0 to 4.5	3.6	80	0.5 to 1.0	2.8 to 4.1
Vandewalle and Mortelmans ¹⁶	2	R	200	200	300	2.5 to 3.5	3.1	110 to 112	0.75	3.5 to 4.7
Wu and Han ¹⁷	4	I	170 to 230	50	315 to 397	4.0	12.5 to 15.3	144 to 152	1.0 to 3.0	8.8 to 15.1
Dancygier and Savir ¹⁸	2	R	200	200	273	2.7	3.5	109 to 111	0.75	3.7 to 3.8
Fehling and Thiemicke ²⁰	3	I	200	30	300	4.0	21.8	186 to 208	1	11.1 to 12.7
Shoib ²¹	1	R	300	300	920	3.0	2	80	1	2.3
Spinella et al. ²²	2	R	150	150	219	2.0 to 2.8	1.9	80	1	3.5 to 4.3
Yang et al. ⁸	6	I	500	50	640	2.5 to 3.4	6.8	169 to 193	1.0 to 2.0	8.7 to 19.2
Aziz and Ali ²³	4	R	120	120	150 to 270	1.0 to 2.0	3.9 to 4.0	135	0.4	5.3 to 14.7
Cuenca ²⁴	4	I	130	90	308	2.9	3.7	84 to 96	0.63	2.3 to 4.0
Rawashdeh ²⁵	4	R	120	120	188	2.2 to 3.3	5.6	95	0.4 to 1.2	3.9 to 6.6
Hong et al. ¹⁰	9	I	250	40	445 to 625	2.5 to 3.5	15.9 to 22.3	160 to 170	1.0 to 1.5	13.9 to 25.1
Mészöly and Randl ²⁹	6	I	200	60	314	3.5	11.7	160 to 188	1.0 to 2.0	10.6 to 19.0
Bermudez and Hung ⁵	21	R	165	165	260	1.5 to 3.3	7.6	94 to 136	0.75 to 2.25	4.0 to 19.0
Yavaş et al. ³²	13	R	100	100	124	4.0	5.1	127 to 140	0.5 to 1.5	2.9 to 5.1
Hung and Wen ³³	7	R	165	165	260	1.5 to 3.3	7.6	91 to 119	0.75 to 1.50	6.4 to 17.8
Jin et al. ³⁴	1	I	300	70	350	2.0	6	106	0.75	9.1
Wang et al. ³⁵	4	R	150	150	199	1.8 to 2.3	6.6 to 8.2	127	2	11.9 to 14.2
Cao et al. ³⁷	5	R	150	150	200 to 219	2.3	4.5 to 8.2	117	2	7.5 to 14.2
Yang et al. ³⁸	8	R	250	250	269 to 280	1.5 to 3.1	5.6 to 7.2	130 to 152	2.65	9.0 to 14.4
Jabbar et al. ³⁹	4	T	350	140	240	2.0 to 3.0	2.9	113 to 127	1	5.4 to 7.4
Total	118	Min.	100	30	124	1	1.9	80	0.4	2.3
		Max.	500	300	920	4.5	22.3	208	3.0	25.1
		Mean	192	126	287	3	7.8	129	1.33	9.8

Note: 1 mm = 0.039 in.; 1 N = 0.225 lb; 1 MPa = 145 psi.

the data set is 129 MPa (18,700 psi), with 23% of the beams exceeding a compressive strength of 150 MPa (22,000 psi). For the reinforcement, the average longitudinal reinforcing ratio ρ of A_s to bd was 4.8%, and the average fiber volume fraction V_f was 1.33%. The fibers used in the beams of the evaluation database included straight steel fibers (50%), hooked-end steel fibers (36%), polyvinyl alcohol (PVA) fibers (3%), and hybrid fibers (11%).

DEVELOPMENT OF PRACTICAL SHEAR STRENGTH EQUATION FOR HS-HPFRC AND UHPC BEAMS

A practical approach that balances simplicity and accuracy was developed to predict the shear strength of HS-HPFRC and UHPC beams without stirrups. The shear strength v_u of the beams is assumed to consist of the shear components from the matrix v_c and fibers v_f as follows

$$v_u = \lambda_s [v_c + v_f] \beta_s \quad (\text{MPa}) \quad (1)$$

$$v_u = \sqrt{1 + \frac{2}{254}} \left[A e \left(f'_c \rho_w \frac{d}{a} \right)^{\text{Exp.1}} + (B v_b)^{\text{Exp.2}} \right] \left(\frac{b}{b_w} \right)^{\text{Exp.3}} \quad (2)$$

where λ_s is size effect factor⁶; β_s is shape factor b/b_w ; e is dimensionless factor that accounts for arching action: $e = 1$ for $a/d > 3.4$ and $e = 3.4(d/a)$ for $a/d \leq 3.4$; a is shear span (mm); d is effective depth (mm); f'_c is cylinder compressive strength (MPa); b is width of the beam for rectangular beams or width of the compressed flange for isolated flanged beams such as I-shaped or T-beams, or $2h_f + b_w$ for intermediate T-beams as per Cladera et al.⁴⁸; b_w is width of the web of the beam (mm); h_f is thickness of the compressed flange (mm); v_b is shear component associated with fibers; and A, B, and Exp. 1, 2, and 3 are empirical coefficients.

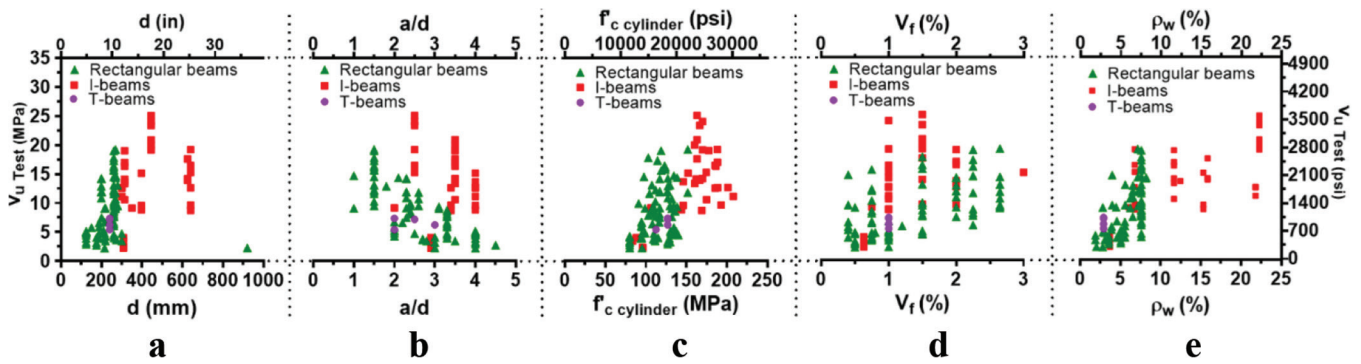


Fig. 1—Distribution of beam shear strengths against different design parameters.

In Eq. (1), the shear component contributed by the matrix v_c is estimated as

$$v_c = Ae \left(f'_c \rho_w \frac{d}{a} \right)^{Exp.1} \quad (\text{MPa}) \quad (3)$$

The combination of the terms e and $f'_c \rho_w (d/a)$ was suggested by Zsutty⁴⁹ based on the results of shear tests on RC beams. It is also employed by Kwak et al.⁵⁰ for estimating the shear strength of steel fiber-reinforced concrete (SFRC) beams.

Narayanan and Darwish⁵¹ defined the fiber contribution to the shear strength of FRC beams in terms of the fiber efficiency factor α , average fiber-matrix bond strength τ , and fiber factor F as

$$v_b = \alpha \tau F \quad (\text{MPa}) \quad (4)$$

The fiber efficiency factor considers the anisotropic properties of FRC and accounts for the effects of fiber distribution and orientation. Based on fracture mechanics, Romualdi and Mandel⁵² derived that the fiber efficiency factor is 0.41 for FRC beams with diagonal shear cracks. Existing studies suggest that $\tau = 4.15$ MPa (600 psi) for steel fibers⁵³ and $\tau = 0.04$ MPa (5.8 psi) for PVA fibers.⁵⁴ Naaman⁵⁵ derived a theoretical model for predicting postcracking tensile strength in FRC using statistical mechanics, taking into account the probabilistic nature of tensile strength and the weakest link hypothesis. In Naaman's⁵⁵ model, the tensile strength of a material is not considered as a volume average quantity, but rather as an extremum quantity. Key factors in Naaman's statistical model for quantifying tensile strength include the distribution of fibers, the aspect ratio, pullout forces, and bond strength deterioration due to fiber density. The fiber factor inferred from Naaman's⁵⁵ tensile strength model can be expressed in terms of the aspect ratio (that is, length to the diameter ratio L_f/D_f) and fiber volume fraction V_f . Narayanan and Darwish⁵¹ modified Naaman's⁵⁵ fiber factor by incorporating a bond factor d_f to consider the bond property of steel fibers as

$$F = \left(\frac{L_f}{D_f} \right) V_f d_f \quad (5)$$

Kwak et al.⁵⁰ proposed that the shear strength contribution of steel fibers in SFRC beams is linearly proportional to v_b , and thus added a modification factor to v_b . They subsequently derived a suitable empirical value for the modification factor based on a database with 139 SFRC beams. Kwak et al.'s⁵⁰ equation gives reasonable beam shear predictions for SFRC.

Based on the cumulative knowledge of the studies,^{50-52,55} the fiber contribution to the shear strength of HS-HPFRC and UHPC beams was suggested in Eq. (6). The proposed equation's applicability was extended to HS-HPFRC and UHPC beams with monofibers or hybrid fibers as shown in Eq. (7) and (8)

$$v_f = (Bv_b)^{Exp.2} \quad (\text{MPa}) \quad (6)$$

$$v_b = 0.41 \sum_{i=1}^n \tau_i F_i \quad (\text{MPa}) \quad (7)$$

$$F_i = \sum_{i=1}^n \left(\frac{L_{f,i}}{D_{f,i}} \right) V_{f,i} d_{f,i} \quad (8)$$

where $L_{f,i}$, $D_{f,i}$, $V_{f,i}$, and $d_{f,i}$ are the length, diameter, fiber volume fraction, and bond characteristic for the i -th type of fibers, respectively; and n is the number of the types of fibers. The bond characteristics for straight steel fibers is 0.5,⁵¹ for crimped fibers is 0.75,⁵¹ for hooked-end fibers is 0.75, for indented fibers is 1,⁵¹ and for PVA fibers is 0.25.

The potential synergetic effect of hybrid fibers⁵⁶ is admittedly ignored in Eq. (7) due to its complex nature and insufficient studies. It is also worth mentioning that both fiber-matrix bond strength τ and the fiber efficiency factor α were derived for conventional FRC materials and their use for UHPC beams should be conservative. This is because the UHPC matrix has a higher bond strength with the fibers due to its high cementitious content. In addition, UHPC usually uses microfibers, which have a higher fiber efficiency than that of the macrofibers used in conventional FRC. Nevertheless, it is considered reasonable to limit the fiber efficiency in one-way shear because there is no structural redundancy.

Placas and Regan⁵⁷ demonstrated the beneficial influence of the flange on the beam's shear capacity due to the applied constraints on the beam web. They proposed that the increase in shear strength due to the presence of beam flanges can be estimated using the cross-sectional shape factor $\beta_s = b/b_w$.

The incorporation of the cross-sectional shape factor β_s in Eq. (1) extends the applicability of the equation to rectangular, flanged, and T-shaped beams.

Minelli et al.⁵⁸ demonstrated that for FRC beams, an increase in the beam effective depth reduced the normalized shear strength. The size effect on the shear failure of HS-HPFRC and UHPC beams is a complex fracture phenomenon, causing a lack of a purely mathematical approach to account for it. Given the quasi-brittle nature of HS-HPFRC and UHPC, the nonlinear fracture mechanics size effect employed by ACI 318-19⁶—that is, $\sqrt{2/(1 + [d/254])}$ —is applied in Eq. (1) as the general approximate mathematical form. The adequacy of the adopted general form is based on the fact that the shear failure pattern of HS-HPFRC and UHPC beams also agrees with two fundamental assumptions identified by Bažant and Yu⁵⁹: 1) the shear failure is caused by cohesive fracture propagation; and 2) the maximum load is attained only after large fracture growth (rather than at fracture initiation).

Equation (2) assembled the parameters with proven influence on the shear strength of FRC beams. The generalized reduced gradient (GRG) nonlinear algorithm, implemented in Microsoft Excel's Solver function, was used to calibrate coefficients using data from the established database. The primary goal of this algorithm was to minimize the objective function, herein defined as the coefficient of variation (COV), calculated as the standard deviation (SD) divided by the mean. The GRG algorithm operates iteratively, recalculating gradients and adjusting step sizes in each step. It mainly focuses on finding the nearest local optimum and employs techniques to potentially improve the chances of identifying a global optimum. The iterative process persisted until predetermined convergence criteria (set by default to 0.0001) were satisfied, culminating in the following proposed shear equation for HS-HPFRC and UHPC beams

$$v_u = \sqrt{\frac{2}{1 + \frac{d}{254}}} \left[2.25e \left(f_c' \rho_w \frac{d}{a} \right)^{0.57} + (1.80 v_b)^{1.3} \right] \left(\frac{b}{b_w} \right)^{0.35} \quad (\text{MPa}) \quad (9)$$

It is interesting to note that the calibration results indicate that the shear component v_b , originally proposed for conventional FRC beams,⁵¹ is magnified by 1.8 times and an order of 1.3 for the HS-HPFRC and UHPC beams. This is likely because the tensile strain hardening behavior and high bond strength between fibers and matrix for HS-HPFRC and UHPC were not taken into account by the direct employment of the fiber-matrix bond strength τ and bond factor d_f suggested for FRC. These factors were intended to be calibrated due to the lack of sufficient experimental data. Notably, all the parameters in Eq. (9) are readily available to structural engineers in the material identity card that is required in UHPC's design guidelines and standards.^{40,41} Rather than the material tensile or bending strength, the equation relies on the material compressive strength. Consequently, it prevents the complex details involved in the uniaxial tensile tests and bending tests, thus reducing the variance in the test results. It is important to note that the ASTM C39 standard practice for

concrete compressive testing applies to UHPC with a minor modification on the loading rate, as stated by ASTM C1856.

EVALUATION OF PROPOSED SHEAR STRENGTH EQUATION

The performance of the proposed shear strength equation for HS-HPFRC and UHPC beams is assessed by comparing its predictions with the solutions obtained by multiple methods, including existing shear strength equations and ML-based models. In addition, the influence of different design parameters on the prediction performance was investigated.

Shear strength models

Development of ML-based shear strength model—Artificial intelligence (AI)⁶⁰ is a promising approach for interpreting shear test data and generating shear equations. Existing studies have derived shear strength equations for FRC by using AI techniques such as genetic algorithm (GA), genetic programming (GP), and multi-expression programming (MEP).⁶¹⁻⁶³ AI-based shear strength equations vary considerably in their expressions to address interactions between design parameters. However, two critical issues emerge with AI-based shear equations. The first is that a reasonable and effective AI-based equation should be developed with sufficient subject matter expertise on concrete materials and structures. Some existing AI-based shear equations were developed by solely focusing on the deployment of AI algorithms without scrutinizing the accuracy of the data sets. For example, failing to compare a beam's flexural capacity with its flexural demand during data cleaning could lead to errors in the shear strength database. This might happen if beams with evident flexure-shear failure or flexure failure are mistakenly incorporated. The second issue is that most AI-based equations are only valid for a limited range of design parameters, which may lead to irrational results if not used carefully. For example, Solhmirzaei et al.'s⁶³ equation predicts negative strength for beams with an a/d greater than or equal to 4. In addition, the equations by Sarveghadi et al.⁶¹ and Solhmirzaei et al.⁶³ predict negative strength when synthetic fibers are used.

This study employed an unexplored path to predict the shear strength of HS-HPFRC and UHPC beams by generating an optimized threshold using supervised learning algorithms with the evaluation database. Three proprietary ML algorithms from the software package TIBCO Statistica⁶⁴ were used to establish the threshold of the evaluation database—namely, support vector machines (SVM), random forest (RF), and artificial neural network (ANN). The supervised learning algorithms had the reported shear strength as the target value and were fed with different sets of design parameters—Set 1: f_c' , v_b , F , a/d , b/b_w , and ρ_w ; Set 2: f_c' , v_b , a/d , b/b_w , and ρ_w ; Set 3: f_c' , v_b , a/d , and ρ_w ; and Set 4: f_c' , v_b , a/d , b/b_w , ρ_w , and λ_s .

Table 3 shows the performance obtained in the evaluation database by the four sets of design parameters. The ANN models used a multi-layer perceptron (MLP) architecture, comprising multiple layers of interconnected artificial neurons. The notation of the ANN models in Table 3

Table 3—Statistical analysis of ML-based algorithms on evaluation database

ML model	Set 1: $f'_c, v_b, F, a/d, b/b_w, \rho_w$			Set 2: $f'_c, v_b, a/d, b/b_w, \rho_w$			Set 3: $f'_c, v_b, a/d, \rho_w$			Set 4: $f'_c, v_b, a/d, b/b_w, \rho_w, \lambda_s$		
	ANN MLP 6-6-1	SVM	RF	ANN MLP 5-11-1	SVM	RF	ANN MLP 4-10-1	SVM	RF	ANN MLP 6-11-1	SVM	RF
Mean	1.02	1.01	0.93	1.02	1.03	0.98	1.02	1.01	0.98	1.02	1.04	0.93
COV, %	16	28	31	16	35	30	17	22	29	15	30	30
AAE, %	13	16	32	13	16	29	13	16	26	12	16	32
R^2	0.94	0.92	0.81	0.93	0.92	0.80	0.93	0.92	0.77	0.95	0.92	0.82

Note: Mean is $v_{u,Test}/v_{u,Predicted}$; COV is standard deviation/mean; $R^2 = R \times R$ where R is coefficient of correlation.

indicates the input, hidden, and output layers. For instance, Set 1’s MLP has an input layer with six neurons, a hidden layer with six, and an output layer with one neuron. The training algorithm used in the ANNs of this study was the Broyden–Fletcher–Goldfarb–Shanno (BFGS), which is a second-order optimization algorithm. The SVM models employed the radial basis function (RBF) as a kernel function to transform the input data into a higher-dimensional feature space. The RF models implemented a hyperparameter that generated random feature subsampling and reached convergence at 100 individual decision trees. To ensure consistent comparisons, a uniform split of 70% for training and 30% for testing across all AI models was adopted. The 70-30 split was implemented as it is commonly chosen in data sets with limited data points due to its balance between training and testing.

The analysis of the results in Table 3 shows that, within Set 4, the ANN MLP 6-11-1 model demonstrated the highest predictive capability and accuracy, evidenced by the lowest spread (low COV and average absolute error [AAE]). This ANN model also had the highest number of neurons in the hidden layer across all parameter sets. When comparing with Set 4, the results indicate that the lack of the size effect factor in Set 1 led to predictions that overestimated the shear capacity of beams with $d \geq 400$ mm (16 in.). Furthermore, a sensitivity analysis demonstrated that the impact of the F parameter in Set 1 was minor due to the inclusion of the v_b parameter. It is interesting to note that compared to Set 4, the exclusion of the size effect factor in Set 2 also decreased the prediction accuracy in beams with $d \geq 500$ mm (20 in.), implying that the ML-based algorithms identified the size effect in the data set. In addition to the size effect, the exclusion of the shape factor in Set 3 also reduced the prediction accuracy compared to Set 4. This shows that the shape factor enhances the applicability of the equation for different cross-sectional shapes. Therefore, the proposed equation’s performance was compared in the later section with the ML-based models developed using Set 4 design parameters.

Existing shear strength equations—The performance of the proposed shear equation is also compared with that of five existing shear equations. It should be noted that international design guidelines, standards, and equations that rely on the tensile strength of UHPC were not evaluated because of the insufficient tensile strength data reported by the studies that constitute the evaluation database. Table 4

summarizes the details of the five shear equations considered in the statistical assessment. The equations of Wang et al.³⁵ and Yang et al.³⁸ were developed for UHPC beams while the other equations were developed for general FRC beams. For the beams with hybrid fibers, the shear components of fibers v_b in Eq. (7) and the fiber factor F_i in Eq. (8) proposed for hybrid fibers were used in the existing shear equations.

Performance of shear strength equations

Table 5 summarizes the statistical performance of the evaluated shear models. The statistics show that the proposed equation outperformed existing shear equations in predicting the shear strength of 118 beams for all the statistical measures, including the mean (1.00), COV (21%), AAE (18%), and R^2 (0.84) values. It is noted that the prediction results of Wang et al.³⁵ and Yang et al.³⁸ equations had good mean accuracy (mean = 1.01 and 1.06, respectively). However, they had relatively low predictive power ($R^2 \leq 0.45$), high variation (COV $\leq 50\%$), and high error (AAE $\geq 39\%$). The FRC equation of Kwak et al.⁵⁰ was somehow too conservative in predicting the shear strength of HS-HPFRC and UHPC beams, with mean = 1.27. In addition, it also had relatively high variability (COV = 36%) and low predictive power ($R^2 = 0.53$). The equation of Arslan⁶⁵ had reasonable prediction performance when all the beams in the data set were considered, but its accuracy was considerably reduced for deep beams with $a/d < 2.5$ (mean = 1.36). The equation of Sarveghadi et al.⁶¹ generally outperformed other existing equations with improved statistical measures, including the mean, COV, AAE, and R^2 values. However, it should be noted that the statistics for this equation represent the prediction of 112 out of the total 118 beams, as it was not applicable for the six beams with PVA fibers. Additionally, the reliability of Sarveghadi et al.’s⁶¹ equation decreased with an increasing a/d .

Figures 2 and 3 compare the influence of different design parameters on the performance of Sarveghadi et al.’s⁶¹ equation and the proposed equation. From the figures, it is evident that while Sarveghadi et al.’s⁶¹ equation cannot reasonably account for the impact of different design factors, the proposed equation adequately accounts for the influence of the beam depth, a/d , concrete strength, fiber volume fraction, and longitudinal reinforcing ratio on the beams’ shear strength. The prediction results for the beams with hybrid steel fibers indicate that Sarveghadi et al.’s⁶¹ equation generally overestimates the shear strength. Conversely, the hybrid

Table 4—Summary of evaluated shear strength equations

Existing shear strength models for FRC, HS-HPFRC, and UHPC members without transverse reinforcement		Modifications in this study for hybrid fibers
Kwak et al. ⁵⁰	$v_u = 3.7ef_{spfc}^{2/3}(\rho_w d/a)^{1/3} + 0.8v_b \text{ (MPa)}$ $e = \begin{cases} \frac{a}{d} > 3.4, \text{ then } 1 \\ \frac{a}{d} \leq 3.4, \text{ then } 3.4 \frac{d}{a} \end{cases}$ $f_{spfc} = f_c' \cdot \text{cube} \sqrt{(20 - \sqrt{F}) + 0.7 + 1.0\sqrt{F}} \text{ and } v_b = 0.4\tau F$	$v_b = v_{b, hybrid} = 0.41 \sum_{i=1}^n \tau_i F_i$ $F = F_{hybrid} = \sum_{i=1}^n \left(\frac{L_{f,i}}{D_{f,i}} \right) V_{f,i} d_{f,i}$
Arslan ⁶⁵	$v_u = \left(0.2(f_c')^{\frac{2}{3}} \frac{c}{d} + \sqrt{\rho_w(1 + 4F)} f_c' \right) \sqrt[3]{\frac{3}{a/d}} \text{ (MPa)}$ <p>where $(c/d)^2 + (600\rho_w/f_c')(c/d) - (600\rho_w/f_c') = 0$</p>	$F = F_{hybrid} = \sum_{i=1}^n \left(\frac{L_{f,i}}{D_{f,i}} \right) V_{f,i} d_{f,i}$
Sarveghadi et al. ⁶¹	$v_u = \rho_w + \frac{\rho_w}{v_b} + \frac{1}{a/d} \left(\frac{\rho_w f_c' (\rho_w + 2) \left(f_c' \frac{a}{d} - \frac{3}{v_b} \right)}{a/d} + f_c' \right) + v_b \text{ (MPa)}$ <p>where $f_c' = 0.79\sqrt{f_c'}$ and $v_b = 0.41\tau F$</p>	$v_b = v_{b, hybrid} = 0.41 \sum_{i=1}^n \tau_i F_i$ $F = F_{hybrid} = \sum_{i=1}^n \left(\frac{L_{f,i}}{D_{f,i}} \right) V_{f,i} d_{f,i}$
Wang et al. ³⁵	$v_u = 0.4f_c' \left(\sqrt{1 + \left(\frac{a}{d} \right)^2} - \frac{a}{d} \right) \text{ (MPa)}$	None (directly applicable)
Yang et al. ³⁸	$v_u = \Psi \left(\frac{1.4}{a/d} + 0.45 \right) K \sqrt{f_c'} \text{ (MPa)}$ <p>where $a/d > 3$, use $\Psi = 0.6$, and $a/d \leq 3$, $\Psi = 1$, $K = [(L_f/D_f)V_f]^{0.2}$</p>	$K = K_{hybrid} = \sum_{i=1}^n \left[\left(\frac{L_{f,i}}{D_{f,i}} \right) V_{f,i} \right]^{0.2}$
Proposed shear design Eq. (9)	$v_u = \sqrt{\frac{2}{1 + \frac{d}{254}}} \left[2.25e \left(f_c' \rho_w \frac{d}{a} \right)^{0.57} + (1.80v_b)^{1.3} \right] \left(\frac{b}{b_w} \right)^{0.35} \text{ (MPa)}$ $v_b = v_{b, hybrid} = 0.41 \sum_{i=1}^n \tau_i F_i$ $F = F_{hybrid} = \sum_{i=1}^n \left(\frac{L_{f,i}}{D_{f,i}} \right) V_{f,i} d_{f,i}$	—

Note: 1 mm = 0.039 in.; 1 N = 0.225 lb; 1 MPa = 145 psi.

Table 5—Statistical analysis of shear strength equations on evaluation database

Strength model	44 beams with $a/d < 2.5$				74 beams with $a/d \geq 2.5$				Evaluation dataset of 118 beams			
	Mean	COV, %	AAE, %	R^2	Mean	COV, %	AAE, %	R^2	Mean	COV, %	AAE, %	R^2
Kwak et al. ⁵⁰	1.13	29	22	0.45	1.35	37	30	0.83	1.27	36	27	0.53
Arslan ⁶⁵	1.36	17	26	0.88	1.03	32	26	0.80	1.16	29	26	0.82
Sarveghadi et al. ^{61*}	1.11	17	15	0.88	1.03	26	22	0.78	1.06	23	19	0.84
Wang et al. ³⁵	1.00	36	32	0.21	1.02	46	43	0.59	1.01	42	39	0.45
Yang et al. ³⁸	0.85	31	35	0.49	1.18	52	49	0.29	1.06	50	44	0.40
ANN MLP 6-11-1	1.01	14	11	0.95	1.03	15	12	0.95	1.02	15	12	0.95
SVM model	1.00	15	12	0.91	1.06	36	18	0.91	1.04	30	16	0.92
RF model	1.12	22	20	0.82	0.82	28	39	0.87	0.93	30	32	0.82
Proposed Eq. (9)	0.95	22	19	0.82	1.03	21	17	0.83	1.00	21	18	0.84

*Statistics of Sarveghadi et al.'s equation were calculated for 41 deep beams, 71 slender beams, and data set of 112 beams.

Note: Mean = $v_{u, Test} / v_{u, Predicted}$; COV is standard deviation/mean; $R^2 = R \times R$ where R is coefficient of correlation.

fiber factor in the proposed equation leads to more reasonable predictions for beams with hybrid fibers.

In comparison with the existing shear equations, all ML-based models showed substantially enhanced prediction performance, especially the ANN and SVM models. Figures 4(a) and (b) illustrate the prediction results obtained from the ML-based models and the proposed equation for the evaluation database. On average, although the RF model only slightly overestimated the shear strength of the test results (mean = 0.93), its predictions had the highest variation (COV = 30% and $R^2 = 0.82$). In contrast, both the SVM and ANN models had enhanced accuracy (mean = 1.04 and

1.02, respectively), and these models also explained the variation in data well ($R^2 = 0.92$ and 0.95 , respectively). Their predictive power is remarkable, considering only a few parameters used in the model and the variety of the test specimens and setups in existing studies. Moreover, the high predictive power also implies that the employed parameters are sufficient to account for the shear strength of HS-HPFRC and UHPC beams. Among the ML-based models, the ANN model fitted the data best as it had the least variation (COV = 15%) and AAE (= 12%).

When compared with ML-based models, the proposed semi-empirical equation also had a satisfactory prediction

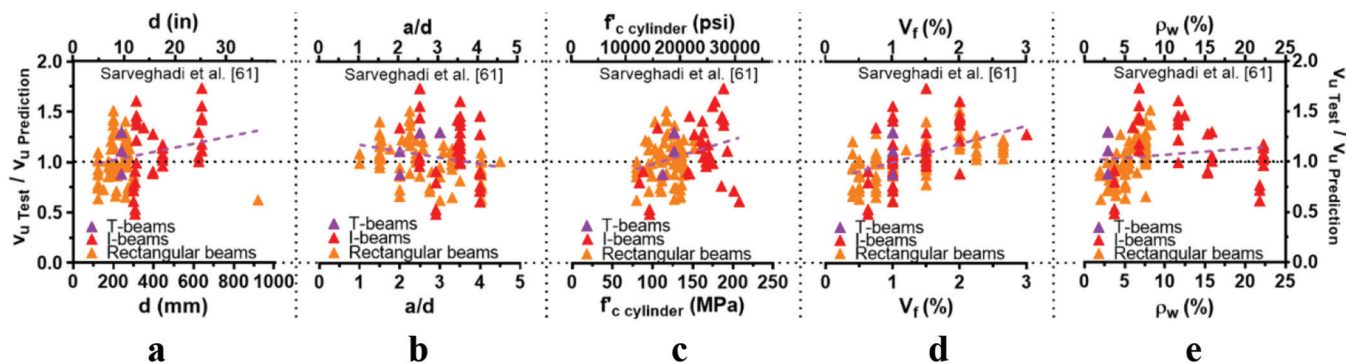


Fig. 2—Influences of different design parameters on performance of Sarveghadi et al.'s equation.⁶¹

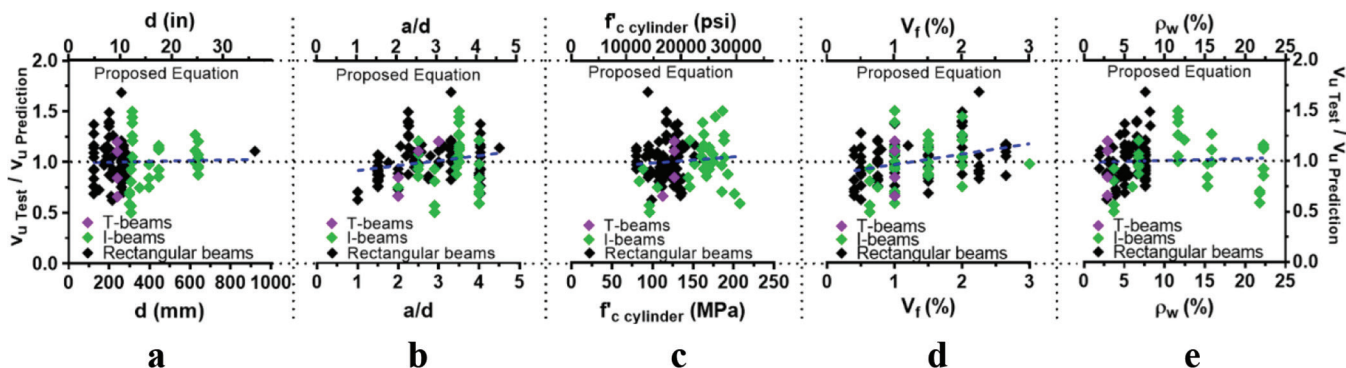


Fig. 3—Influences of different design parameters on performance of proposed equation.

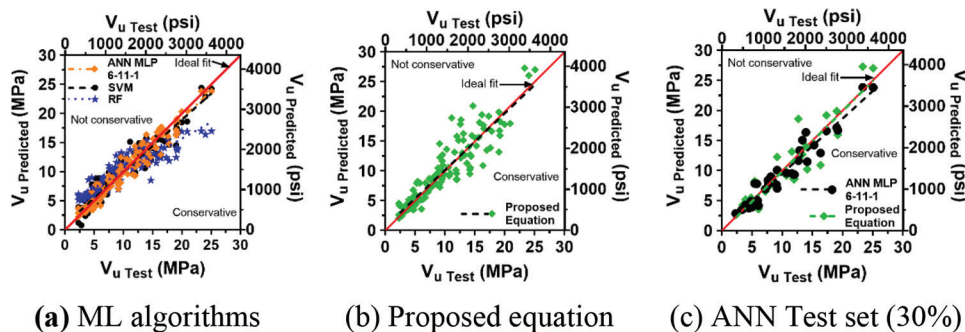


Fig. 4—Experimental shear strength versus predicted shear strength.

accuracy (mean = 1.00) and a high positive correlation with the shear test results ($R = 0.92$). Although its ability to explain the variation in data ($R^2 = 0.84$) is slightly lower than that of the ANN and SVM models, it is considered reasonably accurate given the complexity of the shear failure mechanism. The ANN and SVM models demonstrated high predictive power, due to the inherent strengths of these ML-based models deciphering complex patterns within the evaluation database. Furthermore, ML-based models exhibit a multitude of intricate interactions among the parameters, which impact the prediction power. In contrast, the proposed shear equation presents a simplified closed-form equation that requires only parameters that are readily available in the design phase. Notably, the developed shear equation outperforms the RF model in accuracy and prediction variation.

The predictive performance of the proposed shear equation is further validated by comparing it with the ANN MLP 6-11-1 model, which is the most powerful prediction model evaluated in the study. Figures 3 and 5 show the influences

of the design parameters (including d , a/d , f'_c , V_f , and ρ_w) on the prediction results for the proposed equation and ANN model, respectively. As shown in Fig. 3(a) and 5(a), both the proposed shear equation and ANN model effectively mitigate the impact of the beam depth (ranging from 100 to 1000 mm [3.94 to 39.37 in.]) on the prediction accuracy by using the size effect factor. The prediction accuracy remains stable for the a/d , which varies from 1.0 to 4.5, as depicted in Fig. 3(b) and 5(b). Similarly, stability in prediction accuracy for the compressive strength, ranging from 80 to 200 MPa (12,000 to 29,000 psi), is illustrated in Fig. 3(c) and 5(c). Furthermore, Fig. 3(d) and 5(d) show that both models yield slightly more conservative predictions as the fiber volume fraction increases. The trend lines for the ANN model and the proposed equation both exhibit the highest accuracy at approximately $V_f = 1.5\%$. However, at $V_f = 3\%$, the ANN underestimates the shear strength by 7%, while the proposed equation does so by 14%. Figures 3(e) and 5(e) demonstrate that the accuracy of both equations remained

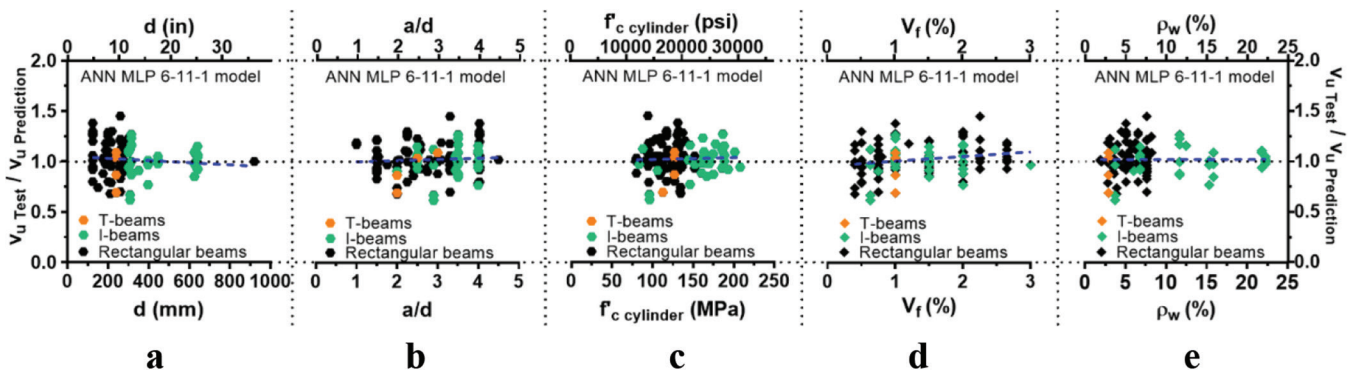


Fig. 5—Influences of different design parameters on prediction accuracy of ANN model.

essentially consistent across various longitudinal reinforcement ratios. It should be noted that in the database used to develop the shear equation, 23 beams (accounting for 20% of the total) featured longitudinal bars with yield strengths ranging from 550 to 900 MPa (approximately 80,000 to 130,000 psi). The shear strength predictions for these beams were only marginally underestimated by the proposed equation, with an average deviation of 8%. This suggests that the yield strength of tensile reinforcement does not significantly impact the shear strength of HS-HPFRC and UHPC beams. Overall, the prediction accuracy of the proposed equation and ANN model remains reasonably consistent. In general, the trend lines on the evaluation data set under varying design parameters are similar in Fig. 3 and 5, indicating that the proposed semi-empirical equation can reasonably emulate the predictions of the ML threshold. Further supporting these findings, Fig. 4(c) offers additional insights into the predictive capabilities of the proposed equation when compared to the ANN model. This figure demonstrates the close alignment of predictions from the proposed equation with the ANN model, underlined by specific metrics: For the proposed equation, the mean is 1.04, COV is 22%, R^2 is 0.86, and R (coefficient of correlation) is 0.93; for the ANN model, the mean is 1.06, COV is 16%, R^2 is 0.93, and R is 0.97. These statistical metrics on the testing set of the ANN model further substantiate the low variation and high accuracy, correlation, and R^2 of the proposed equation, indicating its predictions closely match those of the ANN model.

SUMMARY AND CONCLUSIONS

A practical semi-empirical equation for predicting the shear strength of high-strength high-performance fiber-reinforced concrete (HS-HPFRC) and ultra-high-performance concrete (UHPC) beams without stirrups was developed, using an evaluation shear database with filtering criteria tailored for nonprestressed HS-HPFRC and UHPC beams. This database comprises 118 beams, including 81 rectangular beams, 33 I-shaped beams, and four T-shaped beams. The equation uses common design parameters readily available during the design phase and eliminates the need for uniaxial or flexural tensile test results. Instead, it considers the statistical nature of the impact of fiber reinforcement on shear strength by incorporating fiber content, fiber efficiency factor, fiber-matrix bond strength, and fiber factor. Additionally, the equation accounts for the influence

of the size effect, cross-sectional shape, and hybrid fibers on shear strength. The performance of the equation was validated against existing shear equations and also against three optimized supervised machine learning (ML) models. Key conclusions include:

1. The proposed equation's predictive capability surpassed that of relevant shear equations in prediction accuracy and ability to explain the variance in the data. This is underscored by key metrics, including a mean of 1.00, a coefficient of variation (COV) of 21%, and an R^2 of 0.84.
2. Three distinct artificial intelligence (AI)-based shear strength models, using support vector machine (SVM), random forest (RF), and artificial neural network (ANN) algorithms, were developed using the established database. A consistent split of 70% data for training and 30% data for testing was employed. Statistical analysis revealed that the ANN MLP 6-11-1 model outperformed the others in the evaluation database, as indicated by its overall data set metrics: a mean of 1.02, a COV of 15%, and an R^2 of 0.95.
3. Compared with the AI models, the proposed equation demonstrated enhanced accuracy and predictive variation relative to the RF model. Despite its simplified closed-form expression, the proposed equation achieved predictive power comparable with the threshold established by the ANN MLP 6-11-1 model, as shown in Fig. 4(c).
4. The proposed equation's prediction accuracy remained consistent across varying design variables, including beam depth (100 to 1000 mm [3.9 to 39.4 in.]), a/d (1.0 to 4.5), compressive strength (80 to 200 MPa [12,000 to 29,000 psi]), cross-sectional shapes (rectangular, I-shape, and T-shape), longitudinal reinforcing ratio (0.68 to 8.2), and yield strength of longitudinal reinforcement (414 to 900 MPa [60,000 to 130,000 psi]). Though slightly more conservative with an increasing fiber volume fraction, its accuracy remained reasonable. However, it is important for designers to recognize that, due to the data-driven approach used in deriving the equation, its reliability might be reduced when applied to conditions outside these specified ranges, potentially limiting its applicability and accuracy.

AUTHOR BIOS

ACI member **Manuel Bermudez** is a PhD Candidate in civil engineering at National Cheng Kung University, Tainan, Taiwan. He is a member of ACI Committee 239, Ultra-High-Performance Concrete, and Joint ACI-ASCE Committee 445, Shear and Torsion.

ACI member **Chung-Chan Hung** is a Professor of civil engineering at National Cheng Kung University. He received his MS in mechanical engineering and PhD in civil engineering from the University of Michigan, Ann Arbor, MI, in 2010. His research interests include high-strength reinforced concrete (RC) structures, high-performance fiber-reinforced cementitious materials and structures, and structural retrofitting.

ACKNOWLEDGMENTS

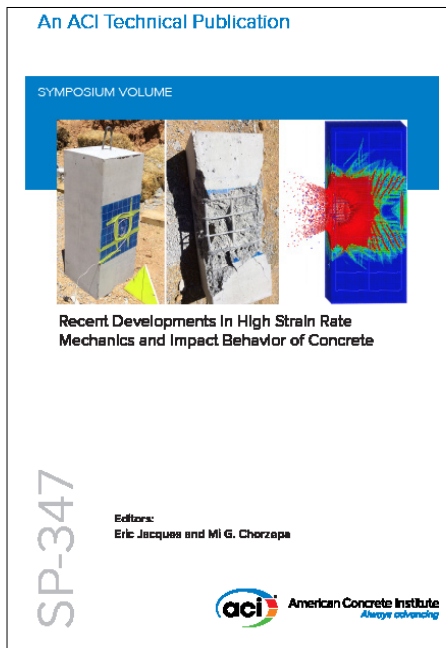
Funding from the National Science and Technology Council, Taiwan (Grant No. 109-2636-E-006-015) partially supported this research. For inquiries, C.-C. Hung, the second author, is the corresponding author. The views expressed are those of the authors and do not reflect the official policy or position of the National Science and Technology Council.

REFERENCES

1. Baby, F.; Marchand, P.; and Toutlemonde, F., "Shear Behavior of Ultrahigh Performance Fiber-Reinforced Concrete Beams. I: Experimental Investigation," *Journal of Structural Engineering*, ASCE, V. 140, No. 5, 2014, p. 04013111. doi: 10.1061/(ASCE)ST.1943-541X.0000907
2. Hung, C.-C.; El-Tawil, S.; and Chao, S.-H., "A Review of Developments and Challenges for UHPC in Structural Engineering: Behavior, Analysis, and Design," *Journal of Structural Engineering*, ASCE, V. 147, No. 9, 2021, p. 03121001. doi: 10.1061/(ASCE)ST.1943-541X.0003073
3. Bermudez, M.; Wen, K.-W.; and Hung, C.-C., "A Comparative Study on the Shear Behavior of UHPC Beams with Macro Hooked-End Steel Fibers and PVA Fibers," *Materials (Basel)*, V. 15, No. 4, 2022, p. 1485. doi: 10.3390/ma15041485
4. El-Helou, R. G., and Graybeal, B. A., "Shear Behavior of Ultra-high-Performance Concrete Pretensioned Bridge Girders," *Journal of Structural Engineering*, ASCE, V. 148, No. 4, 2022, p. 04022017. doi: 10.1061/(ASCE)ST.1943-541X.0003279
5. Bermudez, M., and Hung, C.-C., "Shear Behavior of Ultra-High-Performance Hybrid Fiber-Reinforced Concrete Beams," *International Interactive Symposium on Ultra-High-Performance Concrete*, V. 2, No. 1, 2019.
6. ACI Committee 318, "Building Code Requirements for Structural Concrete (ACI 318-19) and Commentary (ACI 318R-19) (Reapproved 2022)," American Concrete Institute, Farmington Hills, MI, 2019, 624 pp.
7. Voo, Y. L.; Poon, W. K.; and Foster, S. J., "Shear Strength of Steel Fiber-Reinforced Ultrahigh-Performance Concrete Beams Without Stirrups," *Journal of Structural Engineering*, ASCE, V. 136, No. 11, 2010, pp. 1393-1400. doi: 10.1061/(ASCE)ST.1943-541X.0000234
8. Yang, I.-H.; Joh, C.; and Kim, B.-S., "Shear Behaviour of Ultra-High-Performance Fibre-Reinforced Concrete Beams Without Stirrups," *Magazine of Concrete Research*, V. 64, No. 11, 2012, pp. 979-993. doi: 10.1680/mac.11.00153
9. Lim, W.-Y., and Hong, S.-G., "Shear Tests for Ultra-High Performance Fiber Reinforced Concrete (UHPRC) Beams With Shear Reinforcement," *International Journal of Concrete Structures and Materials*, V. 10, No. 2, 2016, pp. 177-188. doi: 10.1007/s40069-016-0145-8
10. Hong, S.-G.; Hong, N.; and Lee, J.-H., "Shear Strength of UHPRC Beams Without Stirrups: Fracture Mechanics Approach," *Shear Strength of UHPRC Beams Without Stirrups: Fracture Mechanics Approach*, Springer, 2018, pp. 447-55.
11. JSCE, "JSCE Recommendations for Design and Construction of High-Performance Fiber-Reinforced Cement Composite with Multiple Fine Cracks," *High-Performance Fiber-Reinforced Cement Composites*, Japan Society of Civil Engineers, Tokyo, Japan, 2008.
12. SIA, "UHPRC—Materials, Design and Construction," Technical Leaflet SIA 2052, Swiss Society of Architects and Engineers, Zurich, Switzerland, 2016.
13. AASHTO T 397, "Standard Method of Test for Uniaxial Tensile Response of Ultra-High Performance Concrete," American Association of State Highway Transportation Officials, Washington, DC, 2022, 49 pp.
14. Ashour, S. A.; Hasanain, G. S.; and Wafa, F. F., "Shear Behavior of High-Strength Fiber Reinforced Concrete Beams," *ACI Structural Journal*, V. 89, No. 2, Mar.-Apr. 1992, pp. 176-184.
15. Shin, S.-W.; Oh, J.-G.; and Ghosh, S., "Shear Behavior of Laboratory-Sized High-Strength Concrete Beams Reinforced with Bars and Steel Fibers," *Fiber Reinforced Concrete Developments and Innovations*, SP-142, J. I. Daniel and S. P. Shah, eds., American Concrete Institute, Farmington Hills, MI, 1994, pp. 181-200.
16. Vandewalle, M. I., and Mortelmans, F., "Shear Capacity of Steel Fiber High-Strength Concrete Beams," *High-Performance Concrete - Proceedings, International Conference Singapore, 1994*, SP-149, V. M. Malhotra, ed., American Concrete Institute, Farmington Hills, MI, 1994, pp. 227-242.
17. Wu, X., and Han, S.-M., "First Diagonal Cracking and Ultimate Shear of I-Shaped Reinforced Girders of Ultra High-Performance Fiber-Reinforced Concrete Without Stirrups," *International Journal of Concrete Structures and Materials*, V. 3, No. 1, 2009, pp. 47-56. doi: 10.4334/IJCSM.2009.3.1.047
18. Dancygier, A., and Savir, Z., "Effects of Steel Fibers on Shear Behavior of High-Strength Reinforced Concrete Beams," *Advances in Structural Engineering*, V. 14, No. 5, 2011, pp. 745-761. doi: 10.1260/1369-4332.14.5.745
19. Son, J.; Beak, B.; and Choi, C., "Experimental Study on Shear Strength for Ultra-High Performance Concrete Beam," *18th International Conference On Composite Materials*, 2011, pp. 3-6.
20. Fehling, E., and Thiemicke, J., "Experimental Investigation on I-Shaped UHPC-Beams with Combined Reinforcement under Shear Load," *Proceedings of HiPerMat*, 2012, pp. 477-84.
21. Shoaib, A., "Shear in Steel Fiber Reinforced Concrete Members Without Stirrups," PhD thesis, University of Alberta, Edmonton, AB, Canada, 2012.
22. Spinella, N.; Colajanni, P.; and La Mendola, L., "Nonlinear Analysis of Beams Reinforced in Shear with Stirrups and Steel Fibers," *ACI Structural Journal*, V. 109, No. 1, Jan.-Feb. 2012, pp. 53-64.
23. Aziz, O. Q., and Ali, M. H., "Shear Strength and Behavior of Ultra-High Performance Fiber Reinforced Concrete (UHPC) Deep Beams Without Web Reinforcement," *International Journal of Civil Engineering*, V. 2, 2013, pp. 85-96.
24. Cuenca, E., *On Shear Behavior of Structural Elements Made of Steel Fiber Reinforced Concrete*, Springer Cham, Switzerland, 2014, 209 pp.
25. Rawashdeh, O. A., "Shear Behavior of Steel-Fiber Reinforced Ultra-High-Strength Self-Compacted Concrete Beams," master's thesis, United Arab Emirates University, Al Ain, UAE, 2015, 164 pp.
26. Abdulhaleq Yaseen, S., "An Experimental Study on the Shear Strength of High-Performance Reinforced Concrete Deep Beams Without Stirrups," *Engineering and Technology Journal*, V. 34, No. 11, 2016, pp. 2123-2139. doi: 10.30684/etj.34.11A.17
27. Manju, R.; Sathya, S.; and Sylviya, B., "Shear Strength of High-Strength Steel Fibre Reinforced Concrete Rectangular Beams," *International Journal of Civil Engineering and Technology*, V. 8, No. 8, 2017, pp. 1716-1729.
28. Qi, J.; Ma, Z. J.; and Wang, J., "Shear Strength of UHPRC Beams: Mesoscale Fibre-Matrix Discrete Model," *Journal of Structural Engineering*, ASCE, V. 143, No. 4, 2017, p. 04016209. doi: 10.1061/(ASCE)ST.1943-541X.0001701
29. Mészöly, T., and Randl, N., "Shear Behavior of Fiber-Reinforced Ultra-High-Performance Concrete Beams," *Engineering Structures*, V. 168, 2018, pp. 119-127. doi: 10.1016/j.engstruct.2018.04.075
30. Pourbaba, M.; Joghataie, A.; and Mirmiran, A., "Shear Behavior of Ultra-High Performance Concrete," *Construction and Building Materials*, V. 183, 2018, pp. 554-564. doi: 10.1016/j.conbuildmat.2018.06.117
31. Ridha, M. M. S.; Sarsam, K. F.; Al-Shaarbaf, I. A. S., "Experimental Study and Shear Strength Prediction for Reactive Powder Concrete Beams," *Case Studies in Construction Materials*, V. 8, June 2018, pp. 434-46.
32. Yavaş, A.; Hasgul, U.; Turker, K.; and Birol, T., "Effective Fiber Type Investigation on the Shear Behavior of Ultra-High-Performance Fiber-Reinforced Concrete Beams," *Advances in Structural Engineering*, V. 22, No. 7, 2019, pp. 1591-1605. doi: 10.1177/1369433218820788
33. Hung, C. C., and Wen, K.-W., "Investigation of Shear Strength of Ultra-High-Performance Concrete Beams Without Stirrup," *Proceedings of the 17th World Conference on Earthquake Engineering*, International Association for Earthquake Engineering, Tokyo, Japan, 2020.
34. Jin, L.-Z.; Chen, X.; Fu, F.; Deng, X.-F.; and Qian, K., "Shear Strength of Fibre-Reinforced Reactive Powder Concrete I-Shaped Beam Without Stirrups," *Magazine of Concrete Research*, V. 72, No. 21, 2020, pp. 1112-1124. doi: 10.1680/jmacr.18.00525
35. Wang, Q.; Song, H.-L.; Lu, C.-L.; and Jin, L.-Z., "Shear Performance of Reinforced Ultra-High Performance Concrete Rectangular Section Beams," *Structures*, V. 27, 2020, pp. 1184-1194. doi: 10.1016/j.istruc.2020.07.036
36. Yavas, A., and Goker, C. O., "Impact of Reinforcement Ratio on Shear Behavior of I-Shaped UHPC Beams With and Without Fiber Shear Reinforcement," *Materials (Basel)*, V. 13, No. 7, 2020, p. 1525. doi: 10.3390/ma13071525
37. Cao, X.; Deng, X.-F.; Jin, L.-Z.; Fu, F.; and Qian, K., "Shear Capacity of Reactive Powder Concrete Beams Using High-Strength Steel Reinforcement," *Proceedings of the Institution of Civil Engineers - Structures and Buildings*, V. 174, No. 4, 2021, pp. 276-291. doi: 10.1680/jstbu.19.00051
38. Yang, J.; Doh, J.-H.; Yan, K.; and Zhang, X., "Experimental Investigation and Prediction of Shear Capacity for UHPC Beams," *Case Studies in Construction Materials*, V. 16, 2022, p. e01097. doi: 10.1016/j.cscm.2022.e01097

39. Jabbar, A. M.; Mohammed, D. H.; and Hamood, M. J., "Using Fibers Instead of Stirrups for Shear in Ultra-High Performance Concrete T-Beams," *Australian Journal of Structural Engineering*, V. 24, No. 1, 2023, pp. 36-49. doi: 10.1080/13287982.2022.2088654
40. AFNOR, "National Addition to Eurocode 2 – Design of Concrete Structures: Specific Rules for Ultra-High Performance Fibre-Reinforced Concretes (NF P18-710)," Association Française de Normalisation, 2016.
41. CAN/CSA A23.1-19/CAN/CSA A23.2-19, "Concrete Materials and Methods of Concrete Construction/Test Methods and Standard Practices for Concrete," CSA Group, Toronto, ON, Canada, 2019, 882 pp.
42. CAN/CSA S6-19, "Canadian Highway Bridge Design Code," CSA Group, Toronto, ON, Canada, 2019.
43. Bencardino, F.; Rizzuti, L.; Spadea, G.; and Swamy, R. N., "Implications of Test Methodology on Post-Cracking and Fracture Behaviour of Steel Fibre Reinforced Concrete," *Composites: Part B – Engineering*, V. 46, 2013, pp. 31-38. doi: 10.1016/j.compositesb.2012.10.016
44. Reineck, K.-H.; Bentz, E. C.; Fitik, B.; Kuchma, D. A.; and Bayrak, O., "ACI-DaFStb Databases of Shear Tests on Slender Reinforced Concrete Beams Without Stirrups," *ACI Structural Journal*, V. 110, No. 5, Sept.-Oct. 2013, pp. 867-876. doi: 10.14359/51685839
45. Reineck, K.-H., and Todisco, L., "Database of Shear Tests for Non-Slender Reinforced Concrete Beams without Stirrups," *ACI Structural Journal*, V. 111, No. 6, Nov.-Dec. 2014, pp. 1363-1372. doi: 10.14359/51686820
46. Peng, F.; Yi, W.; and Fang, Z., "Design Approach for Flexural Strength of Reinforced Ultra-High-Performance Concrete Members Considering Size Effect," *ACI Structural Journal*, V. 119, No. 1, Jan. 2022, pp. 281-294. doi: 10.14359/51734140
47. Graybeal, B., and Davis, M., "Cylinder or Cube: Strength Testing of 80 to 200 MPa (11.6 to 29 ksi) Ultra-High-Performance Fiber-Reinforced Concrete," *ACI Materials Journal*, V. 105, No. 6, Nov.-Dec. 2008, pp. 603-609. doi: 10.14359/20202
48. Cladera, A.; Mari, A.; Ribas, C.; Bairán, J.; and Oller, E., "Predicting the Shear-Flexural Strength of Slender Reinforced Concrete T and I Shaped Beams," *Engineering Structures*, V. 101, 2015, pp. 386-398. doi: 10.1016/j.engstruct.2015.07.025
49. Zsutty, T., "Shear Strength Prediction for Separate Categories of Simple Beam Tests," *ACI Journal Proceedings*, V. 68, No. 2, Feb. 1971, pp. 138-143.
50. Kwak, Y.-K.; Eberhard, M. O.; Kim, W.-S.; and Kim, J., "Shear Strength of Steel Fiber-Reinforced Concrete Beams Without Stirrups," *ACI Structural Journal*, V. 99, No. 4, July-Aug. 2002, pp. 530-538.
51. Narayanan, R., and Darwish, I., "Use of Steel Fibers as Shear Reinforcement," *ACI Structural Journal*, V. 84, No. 3, May-June 1987, pp. 216-227.
52. Romualdi, J. P., and Mandel, J. A., "Tensile Strength of Concrete Affected by Uniformly Distributed and Closely Spaced Short Lengths of Wire Reinforcement," *ACI Journal Proceedings*, V. 61, No. 6, June 1964, pp. 657-672.
53. Swamy, R. N.; Mangat, P. S.; and Rao, C. V. S. K., "The Mechanics of Fiber Reinforcement of Cement Matrices," 1974, pp. 1-28.
54. Hong, L.; Chen, Y.; Li, T.; Gao, P.; and Sun, L., "Microstructure and Bonding Behavior of Fiber-Mortar Interface in Fiber-Reinforced Concrete," *Construction and Building Materials*, V. 232, 2020, p. 117235. doi: 10.1016/j.conbuildmat.2019.117235
55. Naaman, A. E., "A Statistical Theory of Strength for Fiber Reinforced Concrete," doctoral dissertation, Massachusetts Institute of Technology, Cambridge, MA, 1972.
56. Fantilli, A. P.; Kwon, S.; Mihashi, H.; and Nishiwaki, T., "Synergy Assessment in Hybrid Ultra-High Performance Fiber-Reinforced Concrete (UHP-FRC)," *Cement and Concrete Composites*, V. 86, 2018, pp. 19-29. doi: 10.1016/j.cemconcomp.2017.10.012
57. Placas, A., and Regan, P. E., "Shear Failure of Reinforced Concrete Beams," *ACI Journal Proceedings*, V. 68, No. 10, Oct. 1971, pp. 763-773.
58. Minelli, F.; Conforti, A.; Cuenca, E.; and Plizzari, G., "Are Steel Fibres Able to Mitigate or Eliminate Size Effect in Shear?" *Materials and Structures*, V. 47, No. 3, 2014, pp. 459-473. doi: 10.1617/s11527-013-0072-y
59. Bažant, Z. P., and Yu, Q., "Designing Against Size Effect on Shear Strength of Reinforced Concrete Beams Without Stirrups: I. Formulation," *Journal of Structural Engineering*, ASCE, V. 131, No. 12, 2005, pp. 1877-1885. doi: 10.1061/(ASCE)0733-9445(2005)131:12(1877)
60. Naser, M., "An Engineer's Guide to eXplainable Artificial Intelligence and Interpretable Machine Learning: Navigating Causality, Forced Goodness, and the False Perception of Inference," *Automation in Construction*, V. 129, 2021, p. 103821. doi: 10.1016/j.autcon.2021.103821
61. Sarveghadi, M.; Gandomi, A. H.; Bolandi, H.; and Alavi, A. H., "Development of Prediction Models for Shear Strength of SFRCB Using a Machine Learning Approach," *Neural Computing & Applications*, V. 31, No. 7, 2019, pp. 2085-2094. doi: 10.1007/s00521-015-1997-6
62. Shahnewaz, M., and Alam, M. S., "Genetic Algorithm for Predicting Shear Strength of Steel Fiber Reinforced Concrete Beam with Parameter Identification and Sensitivity Analysis," *Journal of Building Engineering*, V. 29, 2020, p. 101205. doi: 10.1016/j.jobbe.2020.101205
63. Solhmirzaei, R.; Salehi, H.; Kodur, V.; and Naser, M., "Machine Learning Framework for Predicting Failure Mode and Shear Capacity of Ultra High Performance Concrete Beams," *Engineering Structures*, V. 224, 2020, p. 111221. doi: 10.1016/j.engstruct.2020.111221
64. TIBCO, "TIBCO Statistica 14.1.0.," <https://docs.tibco.com/products/tibco-statistica-14-1-0>. (last accessed May 20, 2024)
65. Arslan, G., "Shear Strength of Steel Fiber Reinforced Concrete (SFRC) Slender Beams," *KSCE Journal of Civil Engineering*, V. 18, No. 2, 2014, pp. 587-594. doi: 10.1007/s12205-014-0320-x

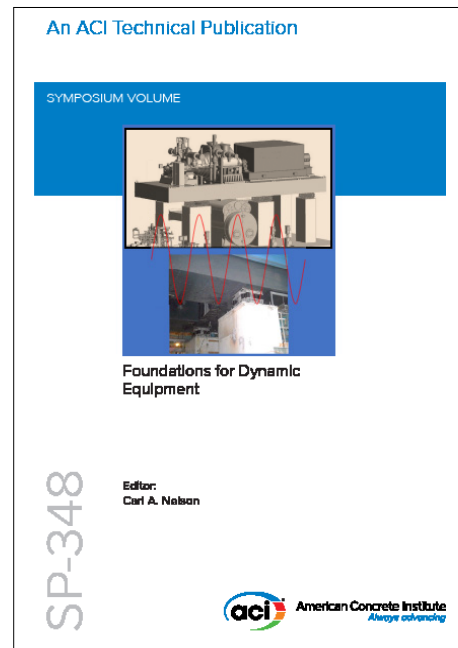
NEW Symposium Publications from ACI



SP-347: Recent Developments in High Strain Rate Mechanics and Impact Behavior of Concrete

This Symposium Volume reports on the latest developments in the field of high-strain-rate mechanics and behavior of concrete subject to impact loads. This effort supports the mission of ACI Committee 370, Blast and Impact Load Effects, to develop and disseminate information on the design of concrete structures subjected to impact, as well as blast and other short-duration dynamic loads.

Available in PDF format: \$69.50
(ACI members: \$39.00) (\$30.50 savings)



SP-348: Foundations for Dynamic Equipment

This special publication grew out of the Technical Session titled “Application of ACI 351-C Report on Dynamic Foundations,” held at the ACI Spring 2019 Convention in Québec City, Québec. Following this event, ACI Committee 351 decided to undertake a special publication with contributions from those session participants willing to develop their presentations into full-length papers. Three papers included in the current publication were contributed by these presenters and their coauthors, with six additional papers provided by others.

Available in PDF format: \$69.50
(ACI members: \$39.00) (\$30.50 savings)



American Concrete Institute

+1.248.848.3700 • www.concrete.org

